7. PELAGIC AND SEA-ICE BIOLOGY – PSB

Hauke Flores[1], Magnus Lucassen[1], Serdar Sakinan[2], Kim Vane[1], Youngju Lee[3], Jannis Hümmling[1], Kamila Faizieva[4], Nils Koschnick[1], Sandra Murawski[1], Martina Vortkamp[1], Insa Kaphegyi[5], Jan Zimmermann[5], Michiel van Dorssen[6];

not on board: Doreen Kohlbach[1], Katja Metfies[1], Barbara Niehoff[1], Fokje Schaafsma[2], Jutta Wollenburg[1], Eun Jin Yang[3], Christoph Stransky[7], Sarah Maes[8], Pauline Snoeijs-Leijonmalm[9]

[1]DE.AWI
[2]NL.WMR
[3]KOR.KOPRI
[4]A.UW
[5]DE.UHH
[6]NL.vDMet
[7]DE.TI
[8]B.EV-ILVO
[9]S.SU

Grant-No. AWI_ AWI_ PS144_06

Objectives

In light of rapid environmental changes in the Arctic Ocean, notably unprecedented ice melt and alterations in oceanic circulation patterns, there is a pressing need to understand the ecosystem dynamics in this remote region. The Central Arctic Ocean Fisheries Agreement (**CAOFA**) emphases the necessity to advance scientific knowledge before considering ecologically sustainable fisheries development. Our expedition ArcWatch-2 is part of the **ArcWatch** campaign in the Central Arctic Ocean (CAO) between 2023 and 2027, as part of the *Programme-Oriented-Research (POF) IV* programme of the Helmholtz association. In order to understand impacts of the climate crisis and predict the future development of the coupled physical-chemical-biological system in the Arctic Ocean, ArcWatch in conjunction with MOSAiC 2019-2020, the approximately 20 Synoptic Arctic Survey (SAS) expeditions 2020-2022, and various observing frameworks by national and international networks (e.g., FRAM, the Nansen Legacy, SUDARCO, Arctic PASSION), aim for systematic interdisciplinary long-term observations in the Arctic Ocean. This is accomplished by sampling of a predefined set of physical, chemical and biological core parameters, applying unified standards and protocols across temporal and spatial scales as part of time series observation in the Arctic Ocean. This approach provides us with adequate information to estimate consequences of the climate crisis on Arctic ecosystems, including the remote CAO.

Besides research related to POF IV, work of parts of the team Pelagic- and Sea-Ice Biology (PSB) is performed under the auspices of the EU-tender *SciCAO* which aims to broaden the knowledge basis on the distribution of fish and their prey in the CAO as part of the Joint Programme for Scientific Research and Monitoring (JPSRM) of the CAOFA. JPSRM-relevant sampling is coordinated with the project Korean Polar Research Institute (KOPRI) programme *Korea- Arctic Ocean Warming and Response of Ecosystem* (K-AWARE) on expedition ARA15B with *Araon* in the Pacific Arctic.

The overarching objective of team PSB is to elucidate the biogeochemical and ecological processes governing primary productivity, biodiversity, trophic interactions and the biological carbon pump within the CAO. Through a systematic interdisciplinary approach integrating physical oceanography, sea-ice physics, marine biology and biogeochemistry we aim to provide crucial insights into the functioning of the unique 3.3 million km^2 ecosystem around the North Pole that until recently was permanently ice-covered. The results of ArcWatch-2 will produce crucial information for the development of effective conservation and management strategies in the CAO. Our expedition aims to achieve the following specific goals:

1. **Collect core parameters of ArcWatch and POF IV for long-term observations:** We will comprehensively assess the biological landscape of the CAO ecosystem, ranging from microbial communities to fish populations, while elucidating trophic linkages and the biological carbon pump. This investigation will encompass sampling of particulate organic matter (POM), ice algae, phytoplankton, zooplankton, protist DNA and cryogenic gypsum across the water column and sea ice habitats. Phytoplankton analysis will be complemented by high-resolution taxonomic analysis from KOPRI.
2. **Investigate the distribution and abundance of fish and their prey in the CAO (SciCAO):** Through a hydroacoustic survey and sampling of fish, zooplankton and metazoan eDNA, we will document the spatial distribution and abundance of fish species within the CAO, along with their associated prey communities. Transcriptomic studies in conjunction with ecophysiological proxies of collected fish in comparison to existing field and laboratory samples will be used to assess the status and adaptational potential of the specimens from CAO. This study will provide essential baseline data for the JPSRM.
3. **Contribute to the record on foraminifera in the changing CAO in relation to paleo-oceanographic sediment records:** By examining foraminifera populations in zooplankton samples collected from the CAO, we aim to compare present changes in relation to past environmental conditions.

Work at sea

The biological and biogeochemical parameters sampled during ArcWatch-2 complement each other for the purpose of obtaining a system understanding of biodiversity and ecosystem functions. They were organised in three closely interconnected work packages (WP).

WP1 ArcWatch core parameters and other POF IV-related sampling

Water column. Using water samples collected with the **CTD rosette**, we sampled POM for various parameters (e.g., carbon, nitrogen, pigments, trophic biomarkers, eDNA for analyses of eukaryotic protist biodiversity, and of metazoan communities; Table 7.1) from different depths, including the subsurface, the chl *a* max, the surface backscatter maximum (SBM, Flores et al. 2023), 50-100 m, the Atlantic Water, and the Arctic Deep Water. The sampled water was filtered on board on appropriate filters, and the filters were stored frozen until analysis in the home laboratories. In addition, eucaryote protist DNA was sampled with an **AutoFIM**, which collected underway-water samples from a seawater intake at about 11 m depth near the ship's bow. Particle distribution in the water column was recorded with an Underwater Vision Profiler (**UVP**). The mesozooplankton community was sampled with a **Multinet** (Hydrobios, 0.25 m^2 opening, 150 µm mesh) at 5 standard depths (1,500-1,000, 1,000-500, 500-200, 200-50, 50-0 m). The Multinet was run in real-time mode using the Deck Command Unit to communicate with the Multinet in order to open the nets manually at depth according to the integrated pressure sensor. Flowmeter readings were recorded for estimations of sampled water volume. Macrozooplankton was sampled with a Rectangular Midwater Trawl (**RMT**). The RMT consisted of a rectangular frame with an effective mouth opening of 8 m^2 (RMT-8) and a 5-mm mesh krill net. A 300 µm zooplankton net with an effective mouth opening of 1 m^2 (RMT-1) initially mounted above the RMT-8 was removed after the first

haul due to handling difficulties. The RMT was equipped with a pressure sensor to record the depth of the net during trawling. A Hydrobios impeller flowmeter was used to estimate the volume of water sampled in m^3. At two ice stations, macrozooplankton was also sampled from 1,000 m to the surface with a 2-m diameter ring net (**MIK net**, 3.14 m^2 opening, 1 mm mesh), but low catch numbers indicated limited functionality of this net. Taxonomic samples from the zooplankton nets were preserved on a 4% formaldehyde-seawater solution, and will later be analysed at AWI with a ZooScan. For trophic biomarker and pollutant analysis bulk stable isotope analysis (BSIA), fatty acid composition and isotopic fractionation (FA-CSIA, Kohlbach et al. 2016), amino acid carbon isotopes (AA-CSIA, Vane et al. 2023), pollutants, macrozooplankton was collected from catches of the RMT net and preserved frozen at -80°C.

Sea ice. On the **sea-ice stations** conducted during ArcWatch-2, we sampled the same general parameters as in the water column by sampling sea-ice cores (Table 7.2). For each ice core, we measured the core length, the ice thickness using a thickness gauge, snowdepth and freeboard. One temperature/salinity (TS), one nutrients, and one cryogenic mineral core were each cut in 10 cm sections. In TS cores, temperature was measured immediately after retrieval of the core at the center of each 10-cm section. Salinity and nutrients were measured after melting at room temperature in darkness on board. From cores sampled for cryogenic minerals, 10-cm sections were processed immediately after the ice station, according to the SOP for cryogenic minerals. A core for Raman analysis and an archive ice core were transported frozen at -20°C back to AWI. For ecological parameters, 6 to 12 “ECO” cores were collected for analysis of pooled samples. The ECO cores were sectioned in 4 sections: bottom 10 cm, bottom center piece, top center piece and top 10 cm. The corresponding sections of all ECO cores were pooled together in polyethylene barrels. On the ship, we added 500 ml filtered seawater (0.2 µm pore size) per 10 cm ice core to each ECO core section barrel, and let the ice cores melt in darkness at 4°C. To accelerate melting, the barrels with center pieces were melted at room temperature. Under-ice water and, after melting (24-48 hours after each ice station), ice core water was filtered for the different parameters. For the same parameters as the ice cores and CTD water samples, we collected under-ice water from the ice-water interface (IWI) and, where present, meltponds using a simple peristaltic pump, and from the SBM using a Niskin bottle with a messenger. To document the procedure, an updated SOP for sea ice samples was created based on the SOPs of the Nansen Legacy, MOSAiC and SAS2021 Oden expeditions.

In addition, we sampled polar cod *Boreogadus saida* and other under-ice fauna with a Surface and Under-Ice Trawl (**SUIT**). The SUIT was equipped with two separate nets besides each other: a 300 µm mesh zooplankton net with a mouth opening of 0.4 x 2 m, and a 7mm half-mesh shrimp net with a mouth opening of 1.6 x 2 m. A sensor array consisting of a CTD (Sea & Sun) with integrated fluorerscence probe and altimeter, a Nortek Aquadopp ADCP, two RAMSES hyperspectral probes (TriOS) to estimate ice algae biomass, and a GoPro camera enabled the recording of environmental data profiles. Sampling profiles were defined as the period between the time that the towing cable was deployed to the desired length (100-150 m), and the time when we started hauling the SUIT back to the ship. Current speed data from the ADCP was used to estimate the distance and area sampled by multiplying average current velocity with the duration of each profile and the width of the SUIT.

To calibrate ice-algae biomass estimates from hyperspectral profiles of the SUIT sensors, we conducted L-arm measurements on the ice with a hyperspectral Ramses sensor during the sea-ice stations (Castellani et al. 2020). At seven ice stations, we performed measurements of under-ice light spectra (300-900 nm) with an l-arm. At each l-arm deployment, we conducted 3 spectral measurements, and collected three ice cores corresponding to each exact light spectrum measurement point. The ice cores were each melted completely according to the SOP for the ECO cores. At the AWI, filters will be analyzed for chlorophyll *a* content using HPLC. In combination, under-ice spectral measurements and their corresponding chlorophyll *a* concentration will be used to generate a model which allows to infer chlorophyll *a* content in

sea ice from under-ice spectral profiles obtained from the spectral sensors mounted on the SUIT.

WP2 SciCAO sampling

Hydroacoustic survey. The EU-project *SciCAO* aims to contribute to baseline knowledge on the distribution of fish in the CAO and the ecosystem supporting it. *SciCAO* sampling was therefore complementary to the ArcWatch core parameter sampling, and results will be obtained in combined analysis of both sets of parameters.

The distribution of fish and its zooplankton prey in the water column was measured continuously throughout the expedition with the **EK80** echosounder of *Polarstern*. The EK80 provides continuous profiles of hydroacoustic backscatter at 38, 70, 120 and 200. These four frequencies were calibrated and operated in broadband mode throughout the expedition with following pulse settings:

Pulse type: LFM up

Pulse Duration: 2.048 ms

Power (W) : Maximum for each channel

Spectra (Start – End frequencies) : Maximum bandwidth

Ramping: Fast

The effective target detection ranges of these 4 frequencies are different, particularly with respect to fish. For example, while 38 kHz provides good signal quality down to 600 m for a wide size range of most fish targets and large macrozooplankton. This effective range (signal to noise ratio or SNR) decreases with increased frequency, therefore recording ranges were adjusted individually per each channel such that:

For 38 and 70 kHz: 800m

For 120 kHz : 400m

For 200 kHz : 250 m

Data was recorded directly to the mass data management system (MDM) through the network, initially as 200 MB then 2 GB packages. 200 MB limit results in a separate file for each minute of data. It was suspected that creation of such high number of files can result in software crash time to time, therefore larger file size found to be more convenient. The EK80 survey was conducted according to the SOP established for JPSRM sampling during the *European Fish Inventory of the Central Arctic Ocean* (EFICA) project (2019-2023; Snoeijs-Leijonmalm et al. 2021). The EK80 was calibrated using an underwater robot positioning a calibration sphere according to a method established during MOSAiC (Snoeijs-Leijonmalm et al. 2022b).

Fish sampling. In order to estimate abundance and biomass of fish and zooplankton from acoustic backscatter data, it is necessary to know the species composition and size distribution of animals in the water column. While the size range of zooplankton is covered by the net sampling of the ArcWatch core parameters, the pelagic fish community on Transect III was sampled with a **pelagic fish trawl**, wherever ice conditions allowed. The pelagic trawl targeted the Atlantic Water layer near the North Pole and in the Eastern Amundsen Basin (100-600 m depth, where most fish are expected to occur (Fig. 2; Snoeijs-Leijonmalm et al. 2022b), as well as hitherto not sampled areas in the Makarov Basin west of the Lomonosov Ridge. Pelagic fish were also sampled with **longlines** from sea-ice stations, following EFICA SOPs (Snoeijs-Leijinmalm et al. 2021). To this end, baited longlines were deployed through a hole in the ice, and at least 200 m away from the ship and any other installations with deep-hanging wires at the earliest possible moment prior to the commencement of an ice stations, and recovered at the latest possible time. The presence of fish in the water column was further investigated by means of metazoan **eDNA** sampled near the surface, in the Atlantic Water layer, and below the AW. On an opportunistic basis, we deployed **baited traps** to sample ice amphipods and polar cod (Snoeijs-Leijonmalm et al. 2022). Additionally, a conventional fyke net was deployed

directly under the ice at three ice stations. The fyke consisted of a stainless-steel half-circle opening (about 1,4 x 1,0 m) equipped with two floating bodies and 7 consecutive plastic rings of decreasing size, resulting in a length of about eight meters including the cod end. For use under the ice the fyke was modified by balancing the floating bodies with a respective counterweight of each ring. The opening was weighted down so that it could first sink under the ice where the fyke could extent in the current, and was finally hauled up and fixed under the ice. Both, traps and fykes were baited with fermented fish byproducts and additionally (on the final station) with smashed amphipods caught BY the SUIT and RMT, respectively.

Fish caught were dissected on board in order to obtain samples for diet, otolith analysis, trophic biomarkers, fecundity, physiological condition, transcriptomic analyses, and population genomics. These samples were preserved according to their EFICA SOPs (Snoeijs-Leijonmalm et al. 2021), and will be analysed in the home laboratories of the SciCAO partners. eDNA sequences will be analysed from the COI, 12S, 16S and 18S amplicons, and metazoan species composition will be obtained from international reference databases (e.g. MIDORI). Polar cod will be targeted with a new specific primer from the mitochondrial D-loop region, allowing for analysis of spatial patterns in relative abundance (Kawakami et al. 2023). For the estimation of the field metabolic rate (FMR) during the life history of the caught fish based on otolith calcium carbonate $\delta^{13}C$ values (Trueman et al. 2023), we will also sample the $\delta^{13}C$ of dissolved organic carbon (DIC) in the water surface and column, and the under-ice habitat.

WP3 Other project-based sampling

Eukaryote protist DNA diversity. We collected protist DNA samples from sea-ice and pelagic samples to characterize the eukaryotic microbial community composition to address the dynamics of the cryo-pelagic coupling in biodiversity in autumn with special emphasis on the re-freezing. These data will be used in combination with data collected within the framework of FRAM and MOSAiC to infer on linkages between sea-ice coverage and eukaryotic microbial biodiversity. This information is part of the INSPRIES PhD project of Jannis Hümmling and the EU-Project **OBAMA_Next** to develop species distribution models that will eventually suggest scenarios for eukaryotic microbial biodiversity, dynamics and distribution in a seasonally ice-free Arctic Ocean.

Phytoplankton diversity. We studied the influences of changes in sea ice melting and oceanic circulation patterns on the phytoplankton community distributions. To understand the ecosystem response in the pan-Arctic region, sampling conducted during the ArcWatch-2 expedition in the Atlantic Arctic Ocean will be compared with those obtained through the **K-AWARE** expedition in the Pacific Arctic Ocean. Ice algae were collected from sea-ice cores and will be analyzed using microscope in a laboratory after the cruise. Phytoplankton will be analyzed at KOPRI using IFCB. To calibrate the results of IFCB, samples for microscopic analysis, photosynthetic pigment concentration, and picophytoplankton abundance were collected for analysis in the laboratory using microscopy, HPLC, and flow cytometer, respectively.

Trophic biomarkers and pollutants. To elucidate trophic relationships and dependencies within the lower trophic food web of the CAO under current environmental conditions, samples of ice algae (ice corer), phytoplankton (CTD), zooplankton (different nets; WP1) and fish (pelagic trawl, SUIT; WP2) were collected for analysis of biomolecules that can be used for indicating the trophic transfer of carbon from under-ice and pelagic primary producers to higher trophic levels. This included the relative composition of fatty acids and highly branched isoprenoids, and isotopic ratios of bulk organic material, fatty acids and amino acids. The main objective was to quantify the dependency of the food web on ice algae *vs.* specific phytoplankton groups, and trace the transfer of these carbon sources to zooplankton and fish. To simultaneously identify the pollution burden of the lower trophic food web, major contaminants (POPs, PFAS) will be identified and quantified in the same species. Collected samples will contribute to the Helmholtz Young Investigator project ***Double-Trouble*** aiming at understanding the trophic

structure of the CAO food web under cumulative stress from warming and (increasing) anthropogenic pollution. The samples will complement samples of the same parameters collected during a CAO expedition in July/August 2024 led by the Norwegian Polar Institute.

Planktonic foraminifera. Planktonic foraminifera were sampled at depth intervals of 1,500-800, 800-100, 100-50, 50-25, and 25-0 meters. Samples from the planktonic foraminifera were stored in 97% ethanol with 2 grams of rose Bengal stain per liter for later analyses at AWI.

Preliminary (expected) results

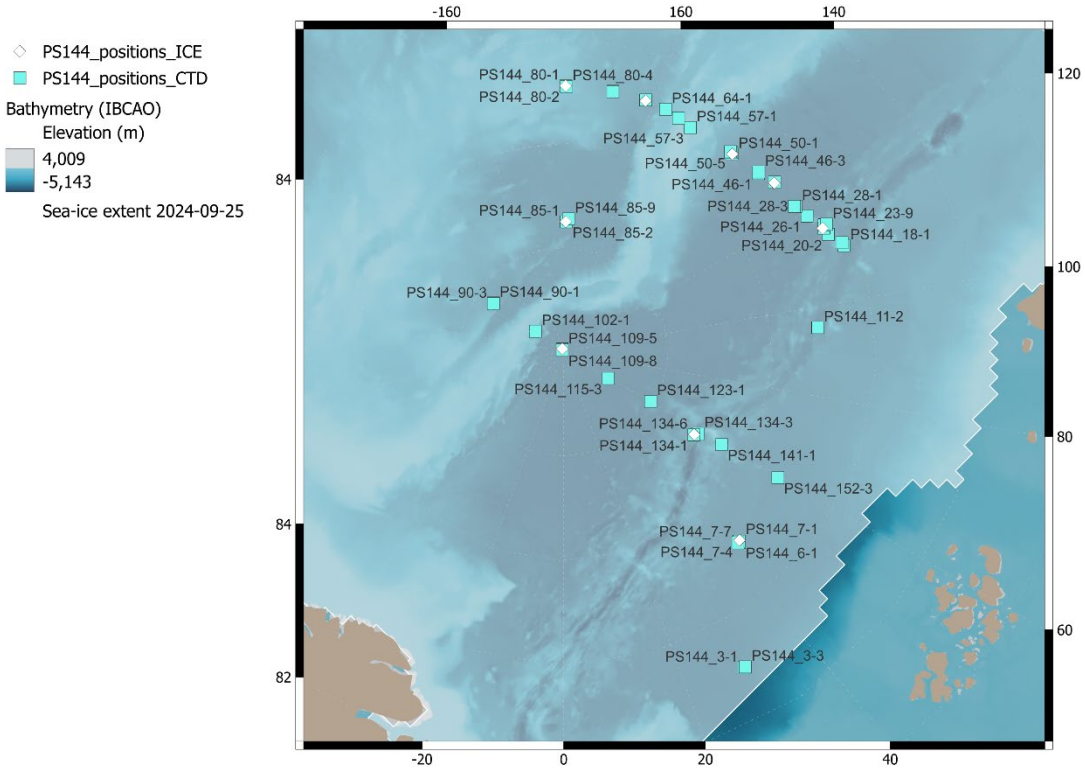

Fig. 7.1: *Distribution of CTD stations and ice stations sampled by team PSB during PS144.*

WP1

CTD sampling. Biogeochemical and ecological parameters were sampled from 46 CTDs at 26 stations during PS144 (Figure 7.1, Table 7.1). The spatial resolution of CTD casts was somewhat denser on Transect III (24 casts) than on Transect II (13 casts), with 9 casts sampled during transit. We collected water samples for the following parameters: pigments, C/N content and stable isotoppes (POC), nutrients, eDNA, protist DNA, and cryogenic minerals. The depth distribution of the sampling of each parameter is shown in Table 7.1. Altogether, we collected 1,142 samples for the WP1 parameters, including metazoan eDNA (WP2), protist DNA and size-fractionated chlorophyll *a*, and cryogenic minerals (WP3).

Tab. 7.1: Summary of biogeochemical and ecological parameters sampled with the CTD during PS144. The numbers indicate the number of sampling sites (stations) at which a parameter was sampled at the respective depth. AA Biom = amino acid biomarkers, Cryog min = cryogenic minerals, Frac Chl *a* = size-fractionated chlorophyll *a* concentration, IWI = ice-water interface, Lip Biom = lipid biomarkers, Metaz eDNA = metazoan eDNA, MP = meltponds, POC = particulate organic matter for C/N content and stable isotope measurements, Prot DNA = DNA samples for protists, SBM = surface backscatter maximum.

Depth feature	Pig-ments	Metaz eDNA	POC	Prot DNA	Frac Chl a	AA Biom	Lip Biom	Cryog min	Total
CTD_surface	22	18	22	22	22			15	26
CTD_Chlmax	22	22	22	22	22	18	18	14	24
Below chl max				20	20				18
CTD_SBM	22	22	21	1	1			17	25
CTD_CDOM_max	1			1	1				1
CTD_50m	22			21	21			1	22
CTD_100m	22			22	22				23
CTD_AW		22	20			18	17	15	26
Below AW		20	20					2	25
CTD_bottom		14						13	18
Unaccounted	1						1		2
Total	**23**	**22**	**22**	**22**	**22**	**18**	**18**	**20**	**26**

UVP casts. The Underwater Vision Profiler (UVP) was deployed a total of 50 times. However, due to low battery voltage in two instances and one malfunction, 47 valid casts were recorded. These casts covered a total water column of 130.117 meters, and 52,479 images were captured (Figure 7.2). The majority of images were taken in transect III (20.402 images, corresponding to 0.33 images per meter), followed by transect II (16,197 images, or 0.37 images per meter) and transect I (4,209 images, yielding 0.56 images per meter).

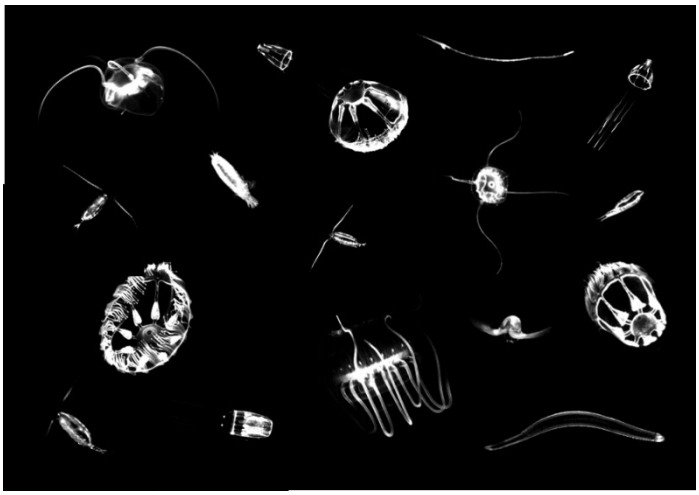

Fig. 7.2: *Example of zooplankton images from the UVP.*

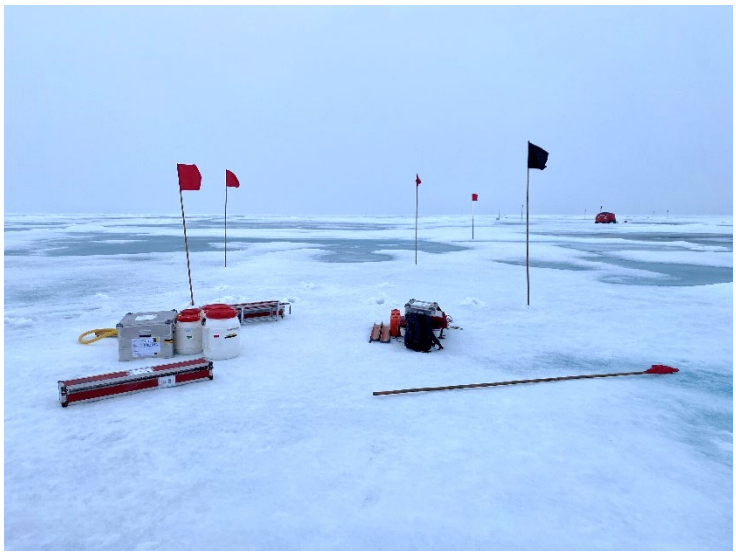

Fig. 7.3: *Example of a coring site (station 23). Foto: ??*

Sea ice stations. Biogeochemical and ecological parameters of sea ice were sampled at nine ice stations (Fig. 7.1, Table 7.2). At each ice station, we selected a coring site at least 100 m from the ship, if visibility was sufient to allow safe working (Fig. 7.3). We collected ice cores for the following parameters: Temperature and salinity (TS), nutrients, cryogenic minerals, Raman analysis, the same biogeochemical and ecological parameters as in the CTD water sampling, and an archive core (Fig. 7.4).

Fig. 7.4: *Example of an ice core for ecological parameters (station 85). All ice cores were photographed for documentation.*

Tab. 7.2: Summary of biological/biogeochemical parameters samples collected during PS144 at ice stations. AA Biom = amino acid biomarkers, Cryog min = cryogenic minerals, Frac Chl *a* = size-fractionated chlorophyll *a* concentration, IWI = ice-water interface, Lip Biom = lipid biomarkers, Metaz eDNA = metazoan eDNA, MP = meltponds, POC = particulate organic matter for C/N content and stable isotope measurements, Prot DNA = DNA samples for protists, SBM = surface backscatter maximum.

device	Depth feature	Pig-	Metaz eDNA	POC	Prot	Frac	NUT	AA Biom	Lip Biom	Cryog min	Total

		ments			DNA	Chl *a*					
Ice corer	sea ice	9	8	9	9	9	9	9	9	8	9
Under-ice pump	IWI	9	7	9	9	9	4	1	1	8	9
	MP	1		1				1			1
	SBM	8	7	8			1				8
Total		**9**	**9**	**9**	**9**	**9**	**9**	**9**	**9**	**9**	**9**

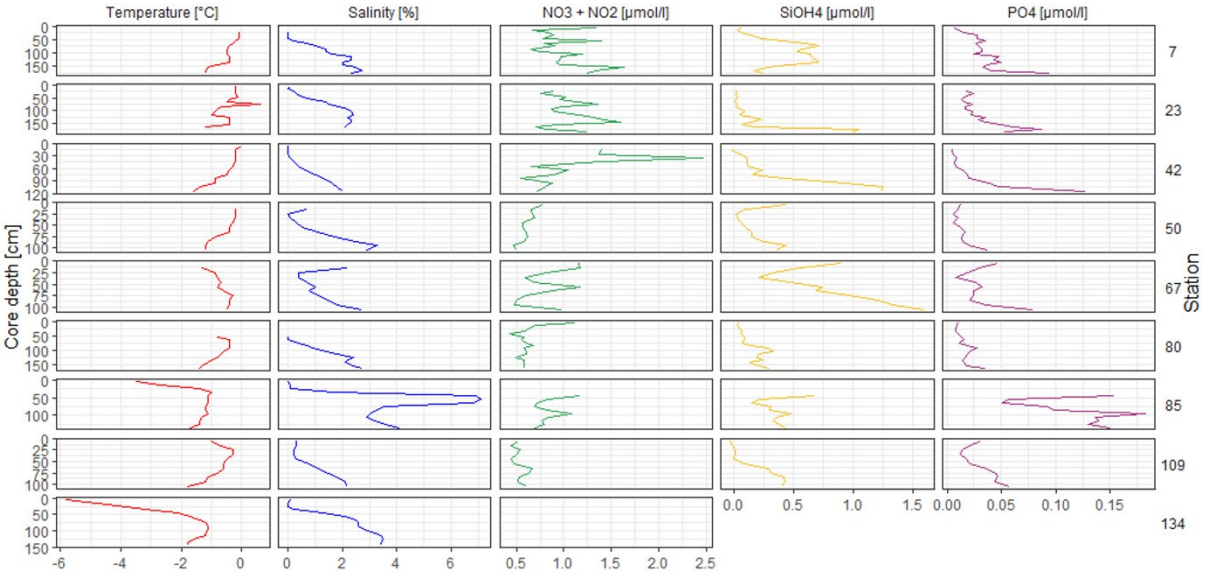

Fig. 7.5: Profiles of temperature, salinity, nitrate + nitrite, silicate and phosphate in ice cores collected during PS144.

Altogether, we collected 160 ice cores from nine ice stations. The majority of the cores was taken on Transect III (Station 23-80). The ice was a mixture of first-year ice (FYI; four stations) and second-year ice (SYI; four stations), with one station at the end of Transect III being multi-year ice (MYI; station 80). The ice average ice thickness was 119 cm (range: 51-194), and the average core length was 124 cm (range: 47-204 cm). Further details are shown in Table 7.3. The temperature- and salinity profiles at the nine sea-ice stations showed a great variety of profile shapes. In the temperature profiles, a seasonal transition from warm surface temperatures at stations 7 to 67 to cold surface temperatures with internal temperature maxima at stations 80-34 was apparent Fig. 7.5. The depth profiles of Nitrate + Nitrite concentrations were highly variable, with no distinct patterns. The highest values were found at station 42, where Nitrate + Nitrite showed a distinct subsurface maximum. Silicate and phosphate values co-varied, with low values near the surface and high values at the ice-water interface at most stations (Fig. 7.5).

Tab. 7.3: Summary statistics of sea-ice sampling sites and ice cores collected during PS144.

Tran-sect	Stn	Ice class	SMB [m]	N	Snow depth [cm]			Ice thickness [cm]			Freeboard [cm]			Core length	
					Mean	Min	Max	Mean	Min	Max	Mean	Min	Max	Mean	Min

T'sit 1	7	SYI	NA	9	1.3	1	3	130.1	110	153	25.6	-2	110	148.3	90
T'sect III	23	SYI	26	17	1.5	1	5	120.4	111	155	13.9	-8	25	150.9	117
	42	FYI	25	14	1.5	1	2	130.8	108	150	16.0	2	32	132.7	109
	50	FYI	25	17	6.3	3	12	93.9	83	102	11.6	5	19	95.9	82
	67	FYI	25	23	5.4	0	12	90.7	51	114	8.8	-6	21	86.6	47
	80	MYI	23	20	5.6	0	11	141.2	116	194	16.4	7	27	144.5	119
T'sit 2	85	SYI	27	20	13.9	10	19	114.8	92	135	9.4	5	16	121.5	88
T'sect II	109	FYI	21	20	24.0	11	32	123.3	114	137	18.5	13	32	115.2	108
	134	SYI	28	20	3.8	3	5	136.6	123	148	15.2	6	25	139.0	123
Total				**160**	**7.8**	**0**	**32**	**119.4**	**51**	**194**	**14.3**	**-8**	**110**	**124.1**	**47**

Multinet. We sampled mesozooplankton at 10 stations, and foraminifera at 8 stations, yielding 50 and 40 samples, respectively (Table 7.4). The mesozooplankton samples will be analysed at AWI with a ZooScan for biomass estimates and diversity.

Tab. 7.4: Summary statistics of Multinet deployments on PS144. Numbers give numbers of stations sampled in each sampling area. Each multinet deployment yielded five zooplankton samples.

Type of multinet	Transit 1	Transect III	Transit 2	Transect II	Total
Mesozooplankton	1	6	1	2	10
Foraminifera	1	4	1	2	8
Total	**2**	**10**	**2**	**4**	**18**

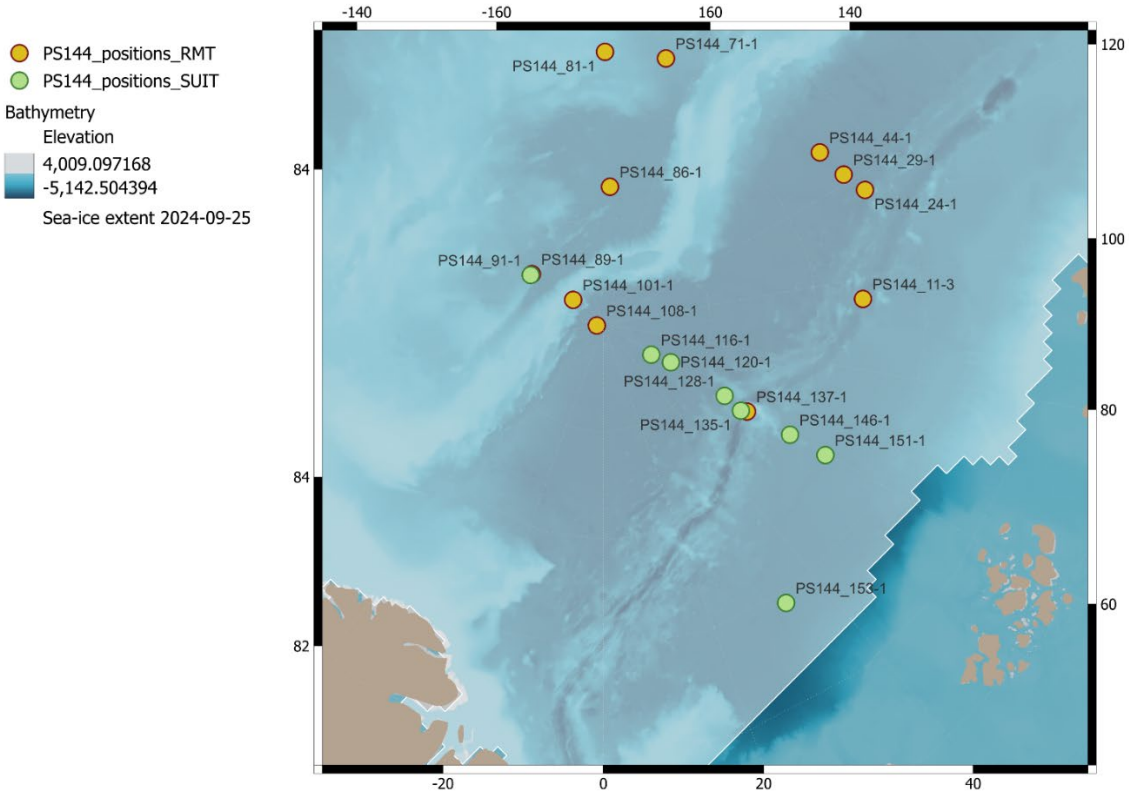

Fig. 7.6: Distribution of RMT and SUIT deployments during PS144.

RMT. The target depth of the RMT deployments was the Deep Scattering Layer (DSL) as identified by the EK80, which was situated between 300 and 450 m. We sampled altogether eleven stations with the RMT. Five stations were sampled on Transect III, three stations on Transect II, and two stations on transits between these transects (Figure 7.6; Table 7.5). The maximum sampling depth ranged between 320 m (station 86) and 700 m (station 137). On three stations (86, 89, 137), the towing wire was caught by sea ice, leading to prolongued trawls and/or greater sampling depth than intended (Table 7.5).

In terms of total abundance of macrozooplankton, station 108 at the North Pole reached the highest values (0.22 ind. m^{-3}). The lowest abundance was recorded at station 81 in the Makarov Basin (0.04 ind. m^{-3}; Figure 7.7). We found at least 30 taxa of macrozooplankton in the RMT samples. At most stations, the taxonomic composition was dominated by chaetognaths, predominantly *Sagitta maxima* and *Pseudosagitta gazellae*. The second most abundant taxon where amphipods, mostly *Themisto* spp. In the Makarov Basin, the ratio between *T. abyssorum* and *T. libellula* was considerably lower than in the Eurasian Basin (Figure 7.7). Conversely, euphausiids (*Thysanoessa* spp.) were more abundant in the Eurasian Basin than in the Makarov Basin. Ctenophores (*Beroe* spp. and *Mertensia* spp.), and the shrimp *Hymenodora glacialis* were sampled at all stations. Three myctophids *Benthosema glaciale* were caught at station 24 and station 89.

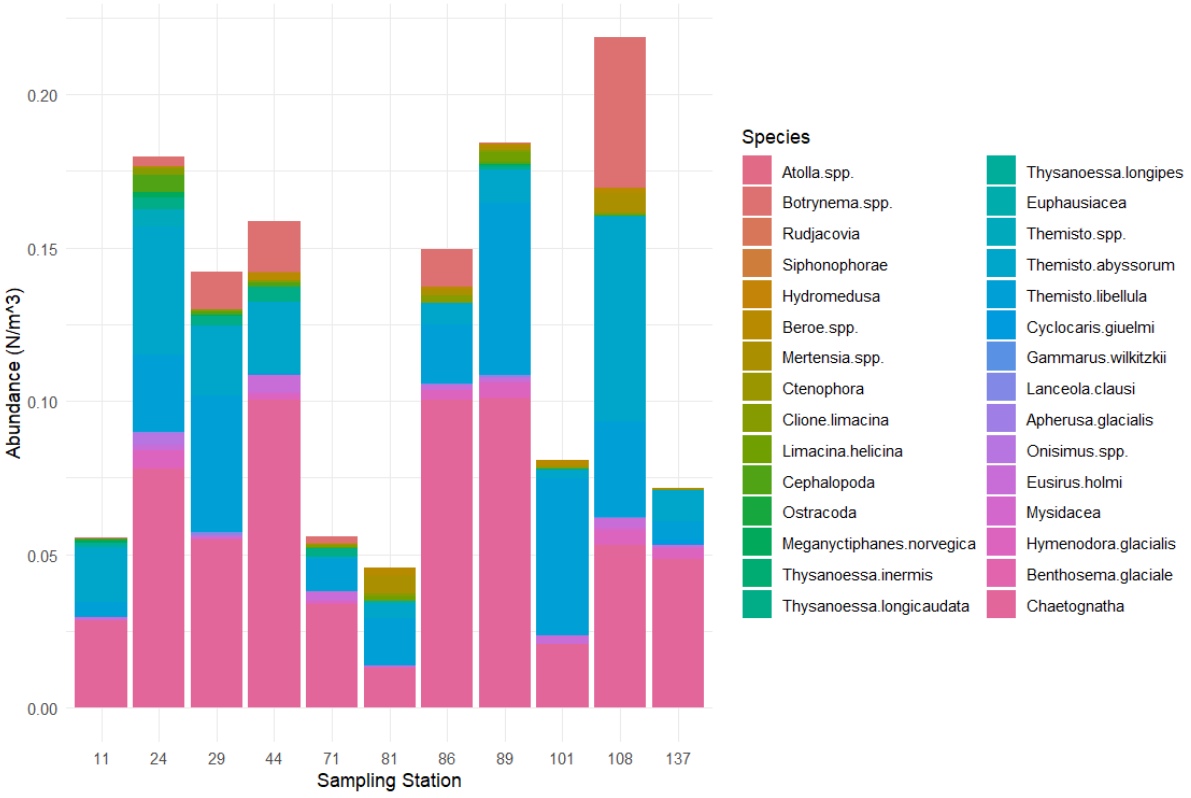

Fig. 7.7: Taxonomic composition of RMT catches during PS144. Abundances relative to sampling effort are expressed in numbers per m^3 of filtered water.

Tab. 7.5: RMT deployments on PS144.

Event	Section	Date	Lati-tude [°N]	Longi-tude [°E]	Target depth [m]	Max depth [m]	Trawl duration [h]	Remarks
PS144_11-3	Transit 1	2024-08-20	85.17	95.52	450	450	0.5	
PS144_24-1	Transect III	2024-08-30	84.55	117.13	450	430	0.5	
PS144_29-1	Transect III	2024-08-31	84.75	121.86	420	447	0.5	
PS144_44-1	Transect III	2024-09-03	84.88	128.40	450	430	0.5	
PS144_71-1	Transect III	2024-09-09	84.94	166.74	350	380	0.5	
PS144_81-1	Transect III	2024-09-11	84.96	179.66	300	324	0.5	
PS144_86-1	Transit 2	2024-09-14	87.45	177.25	300	320	1.3	wire on ice
PS144_89-1	Transect II	2024-09-16	88.38	-124.91	350	465	1.1	wire on ice
PS144_101-1	Transect II	2024-09-17	89.28	-128.68	320	325	0.5	
PS144_108-1	Transect II	2024-09-18	89.87	-77.70	380	395	0.7	
PS144_137-1	Transect II	2024-09-27	86.88	58.66	350	700	1.4	wire on ice

SUIT. The SUIT was deployed on Transect II and Transit 3 only. Deployment sites were chosen with the help of satellite pictures and the ice radar. When drift correction was accurate, satellite pictures considerably improved our ability to identify suitable sampling sites. We sampled eight stations with the SUIT (Figure 7.6; Table 7.6). On three stations, the sampling could not be concluded because the SUIT was damaged by heavy ice (station 91), *Polarstern* got stuck in ice (station 135), or the SUIT was lost (Station 151; Table 7.6). The towing speed during sampling ranged between 0.3 m s^{-1} at station 91 and 1.1 m s^{-1} (0.6 and 2.2 knots) at station 135. The distance sampled ranged between 204 m at station 151 and 1,937 m at station 146. Approximate mean ice draft ranged between 0.6 m at station 151 and 2.2 m at station 135 (Table 7.6). Mean under-ice chlorophyll concentrations ranged between 0.3 µg L^{-1} at station 91 and 0.9 µg L^{-1} at station 121. Details on under-ice water temperature and salinity are shown in Table 7.6.

The catch of the zooplankton net was preserved quantitatively on 4% formaldehyde-seawater solution, and will be analyzed at the AWI. Animals from the shrimp net were enumerated by taxon and sampled frozen for analyses of trophic biomarkers, pollutants and genetics. In terms of total abundance of under-ice fauna from the shrimp net, station 116 near the North Pole reached the highest values (850 ind. ha^{-1}). The lowest abundance (< 50 ind. ha^{-1}) was recorded at station 153 at the end of Transect II (Figure 7.8). We found at least 14 taxa of under-ice fauna in the shrimp net samples. The taxonomic composition was dominated by amphipods, predominantly *Themisto libellula, Apherusa glacialis* and *Eusirus holmi* (Figure 7.8). Interestingly, we found one undidentified benthic polyhaete at station 128. Altogether 14 Polar cod were caught at stations 91 and 128-151.

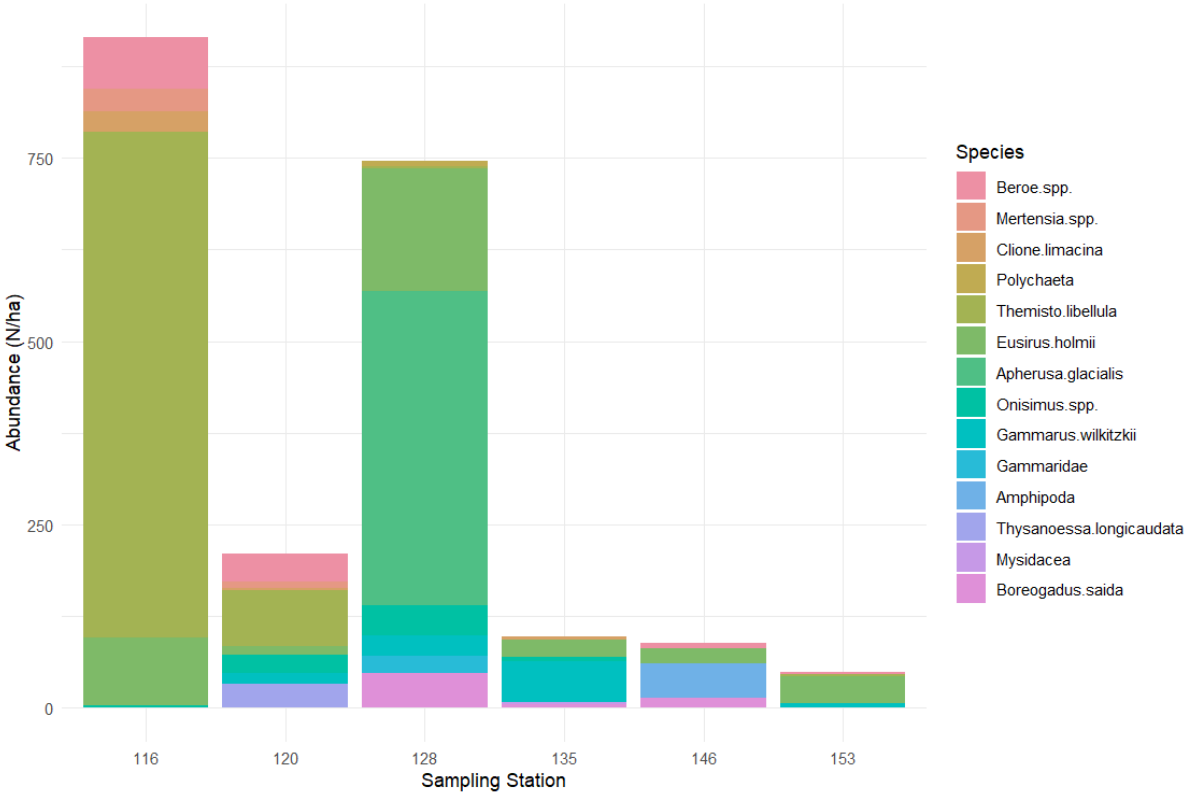

Fig. 7.8: *Taxonomic composition of SUIT catches during PS144. Abundances relative to sampling effort are expressed in numbers per ha (1ha = 100*100 m). Data only shown for stations with trawl distances > 300 m.*

Tab. 7.6: SUIT deployments on PS144, Transect II.

Event	**Date**	**Lati-tude [°N]**	**Longi-tude [°E]**	**Dist-ance [m]**	**Draft [m]** (mean ± SD)	**Temp. [°C]** (mean ± SD)	**Salinity** (mean ± SD)	**Remarks**
PS144_91-1	2024-09-16	88.37	-123.98	263	1.9 ± 0.5	-1.67 ± 0.002	30.5 ± 0.1	SUIT damaged
PS144_116-1	2024-09-21	88.95	57.42	1322	0.7 ± 0.1	-1.71 ± 0.002	31.2 ± 0.1	
PS144_121-1	2024-09-22	88.56	60.47	1858	0.7 ± 0.2	-1.71 ± 0.001	30.9 ± 0.3	
PS144_128-1	2024-09-24	87.39	59.38	1711	1.3 ± 0.7	-1.80 ± 0.001	32.5 ± 0.9	
PS144_135-1	2024-09-25	86.99	57.81	903	2.2 ± 1.8	-1.80 ± 0.002	32.4 ± 0.2	SUIT stuck in ice
PS144_146-1	2024-09-29	85.98	59.34	1937	1.7 ± 0.9	-1.81 ± 0.002	32.8 ± 0.3	
PS144_151-1	2024-09-30	85.22	59.46	204	0.6 ± 0.3	-1.81 ± 0.003	26.9 ± 0.4	SUIT lost
PS144_153-1	2024-10-03	83.82	33.25	1530	N/A	N/A	N/A	

WP2

EK80. The Simrad EK80 echosounder was calibrated at the beginning of the survey and operated continuously throughout the expedition. The ping rate was adjusted to cover a maximum range of 800 m, although the full water column depth often exceeded this range. This limit was set because horizontal resolution depends on the ping rate (number of pings per unit time). The ping rate is primarily constrained by the observation range, as each new pulse can only be transmitted after the previous pulse has traveled to the maximum range and returned. For instance, if the observation range is set to 1,500 m, a delay of at least two seconds is needed before the next pulse can be sent. For this expedition, the maximum observation range was set at 800 m, and the ping interval was adjusted between 1.5 and 1.8 seconds to maximize horizontal resolution. However, when false bottom echoes occurred, the ping rate was modified to keep these disturbances outside the observation range.

For this expedition, a decision was made to use broadband, frequency-modulated (FM) signals instead of narrowband, continuous wave (CW) signals. This choice significantly improved range resolution, enabling fine-scale detection and characterization of individual fish. The enhancement is primarily due to the pulse compression technique: a relatively longer pulse is transmitted to increase energy in the water, and frequency modulation allows the returned echoes to be processed into much finer resolution using a matched filter. Although longer pulse durations in this technique improve the signal-to-noise ratio (SNR), they can also create issues when strong and weak targets are close together, as the stronger target's sidelobes may interfere with processing the weaker target. Trials carried out at the beginning of the expedition, testing pulse durations of 1 ms, 2 ms, and 4 ms, showed that 2 ms was optimal and was thus maintained as the standard setting.

In general, these echosounder settings provided adequate resolution to be able to track and follow individual fish. E.g., at least 7 detections from an individual fish at 350 m at a speed of 4 knots (Fig.7.9). The total amount of data collected throughout 50 days (from Svalbard back to Svalbard) was about 20 TB.

Calibration. The calibration was performed while *Polarstern* was anchored in Adventfjorden in Longyearbyen in Svalbard on the night of August 11, 2024 and the early morning of the next day. A small underwater drone was used to deploy and operate the calibration sphere (38.1 mm Tungsten Carbide) from the moon pool of the *Polarstern*. While all 4 frequencies (38,70,120 and 200 kHz) were calibrated in narrow band mode, only 38 khz and 70 kHz were was calibrated in FM mode. While the low visibility in the water and relatively stronger current complicated the work, especially locating the calibration sphere under the transducer and moving the sphere around within the acoustic beam, the calibration was successful with adequate coverage of the beam and qood quality hits and the center of the beam especially necessary for adjusting the gain. A portable CTD was deployed at the same location for the necessary environmental values. While drone calibration proved to be a successful method, the water visibility turned out to an important factor to take into account in future trials.

While initial quality checks verified the validity of the calibration trials, a conclusive analysis was not completed during the expedition. However, a calibration report will be in early 2025.

Tab. 7.7: Summary statistics of EK80 recordings.

Section	Total File size [TB]	Number of Files	Start	End
Transit 1	2.57	13440	8/13/2024 12:00	8/21/2024 15:00
Medivac	2.19	11355	8/21/2024 15:00	8/28/2024 6:00
Transect III	4.63	24143	8/28/2024 6:00	9/12/2024 19:00
Transit 2	1.12	5826	9/12/2024 19:00	9/16/2024 10:41
Transect II	4.89	8876	9/16/2024 10:41	10/1/2024 15:00
Transit 3	0.87	455	10/1/2024 15:00	10/3/2024 12:00

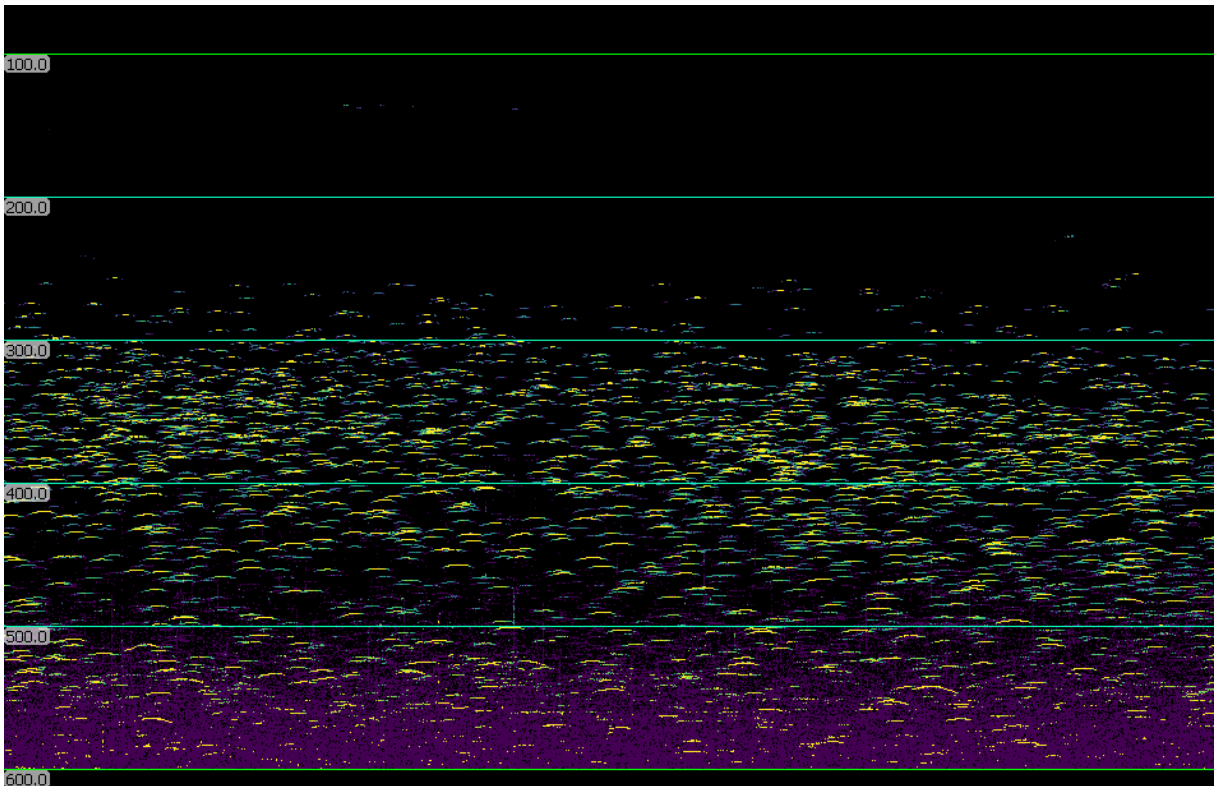

Fig. 7.9: *Sample echogram from one of the pelagic trawl stations (PS144_062). Yellow horizontal lines are indicative of individual targets, most likely Benthosema glaciale.*

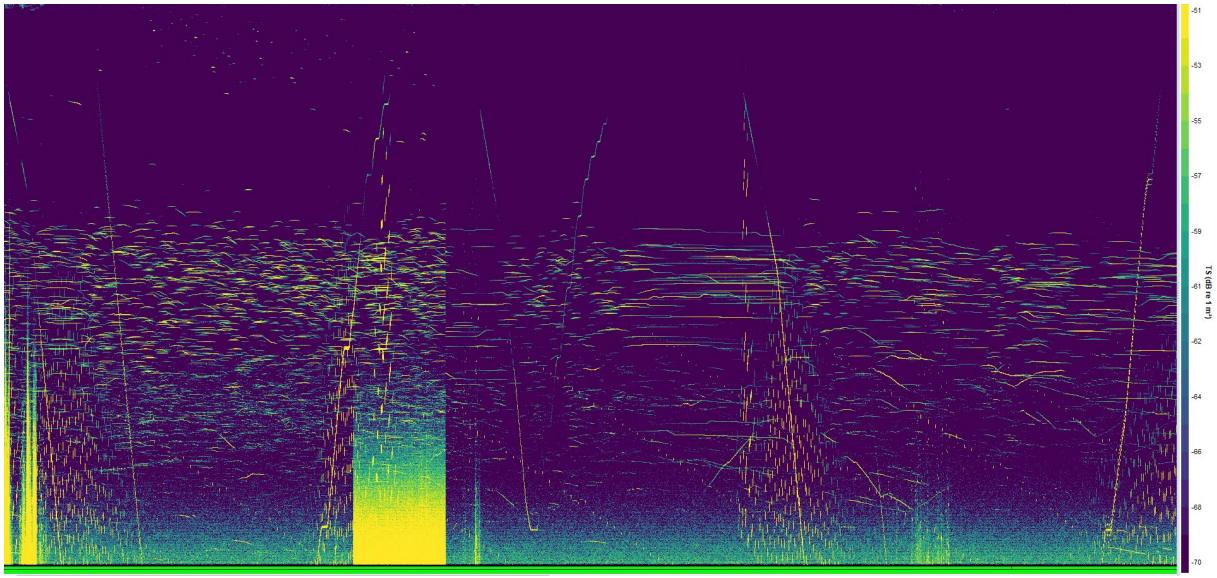

Fig. 7.10: *Sample echogram as an example to illustrate data quality during the CTD station showing a section from surface to 800m. The data was resampled to compress 12 hours section into the same frame. The horizontal marks in the center of the echogram (from ca 300m to 600m) are due to swimbladered fish. The diagonal lines on the echogram show the backscatter from the rosette and the cable. Vertical dashed lines interference from the LADCP running during the CTD deployment. The section towards middle part of the echogram with strong yellow gradient from bottom upwards indicates ship related noise, most likely due to bow thruster.*

While EK80 did not suffer from major noise problems at the stations and in the sections where ship steamed in ice-free waters, at the times when ship was breaking ice, data quality and

representativeness dropped very sharply (Fig. 7.10). In addition to ice-breaking noise, few noise problems were encountered during the stations such as, interference from the LADCP and altimeter sensors from the CTD, bow thruster activity during the stations, and in few occasions the multibeam system. Most of these latter noise sources are in form of spikes and can be dealt with during the post processing. For instance, since the data collected in broadband mode, the ADCP and Multibeam signature can be identified by a spectral analysis and filtered from the data. Some preliminary test with Echoview postprocessing software on board resulted in promising level of cleaning.

Acoustic measurements vs catch. While the number of fish individuals caught by the pelagic net was small, it was considered representative with respect to potential number of fish detected by the EK80 system. Fig. 7.11 illustrates the portion sampled by pelagic trawl relative to the coverage of the acoustic beam.

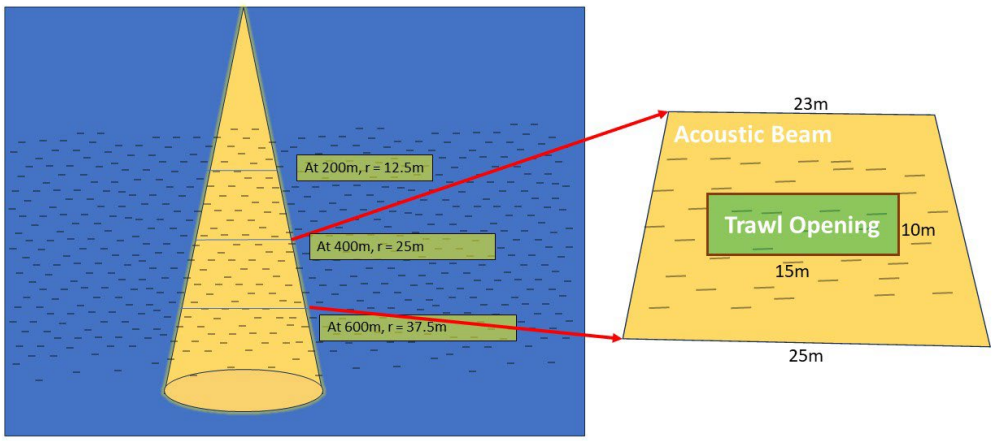

Fig. 7.11: *Volume sampled by pelagic trawl relative to the coverage of the acoustic beam.*

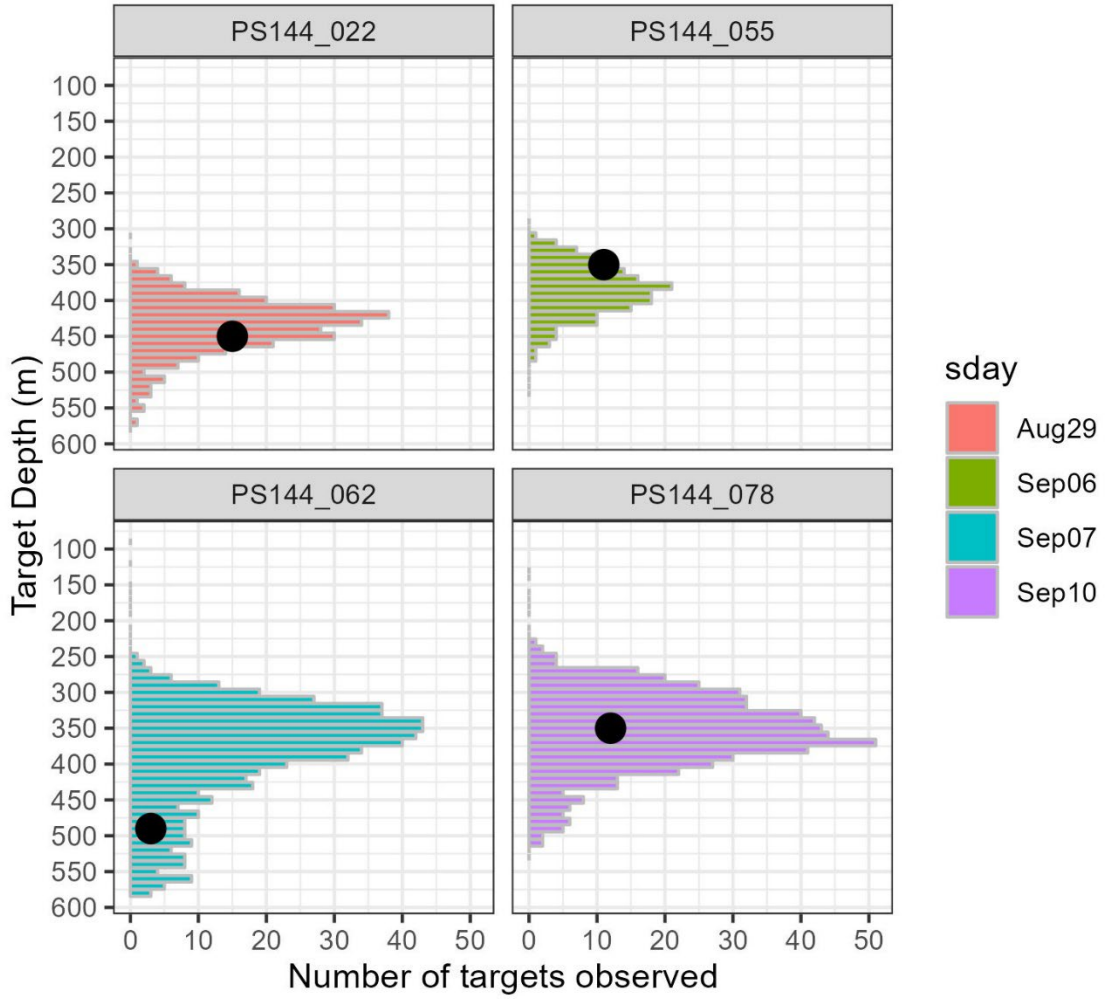

Fig. 7.12: *Number of fish that could have been captured during the trawl sampling vs actual catch.*

Fig. 7.12 provides an approximate illustration of the potential number of fish that could have been captured, assuming a 100% catch efficiency under conditions of such low densities. This estimation indicates that the catch was within the same order of magnitude of echosounder observations. Since the main purpose of the catch was to identify the species/size composition of the echosounder observations (in addition to biological sampling purpose), the small discrepancies are not considered as an issue as the main source of quantitative estimation will be based on the acoustic detections. In addition to that, the catchability is a complex parameter depending on many factors and not necessarily in linear fashion. For example, the herding effect of the net is one important factor in guiding the fish from the mouth of the net towards the center and eventually to the codend. As the front part of the net has larger mesh size exceeding fish size, the herding is especially critical at this stage. It is known that school forming fish consistently exhibit such behavior as a form of predator avoidance. However, in scattered fish in very small densities, such as *Benthosema glaciale* in the Arctic Ocean, it is not well known. Target tracking substantially improves the reliability of the detected targets and accuracy o the estimations. However, such a software module was not available onboard during the expedition. Current estimations of acoustic targets may have resulted in slight over-estimation due to noise which will later be eliminated via target detection.

The consistent DSL as known to occupy the depths from 300 m to 600m from the previous expeditions has been observed continuously during this expedition as well. While the 38 kHz echosounder provided a clear picture of this layer, unfortunately the SNR of the other frequencies including the 70 kHz was not sufficient to cover this range. Therefore 38 kHz is

the only source of information for characterizing the fish distribution. The primary characteristic of this layer was the presence of distinct individual targets with an average TS around -53 dB (SD=1.5). This distribution agrees well with the catches from this depth. During the initial part of the expedition (first half of the expedition), the center of mass was located between the 400-500 m (E.g. PS144_015 and PS144_022). After the first week of September, this layer started to move upwards gradually, reaching almost to 200 m at around North Pole. Near the North Pole we also found the only dense aggregation of potentially larger fish, as observed during MOSAiC leg 1 and leg 5 (station 109; Fig. 7.13). Unfortunately, the sea-ice conditions in this region did not allow to deploy the pelagic trawl. The identity of these strong targets can therefore only be estimated based on our eDNA analysis.

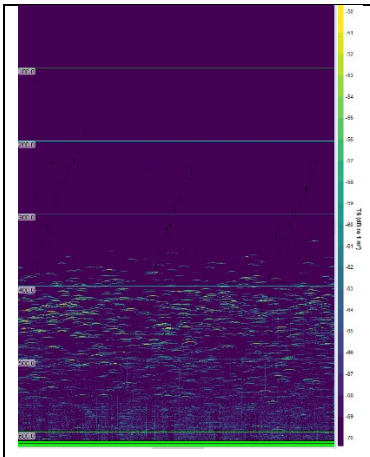

PS144_015 PSN_PS Pelagic Trawl

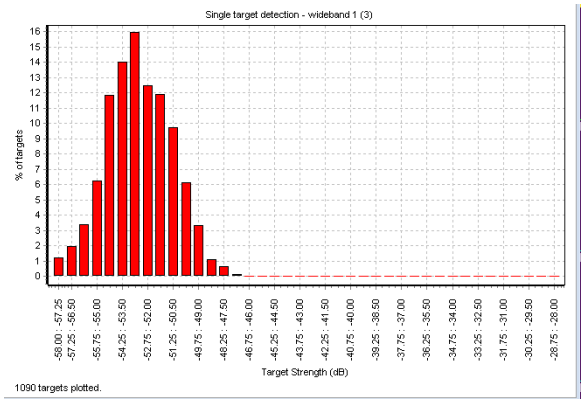

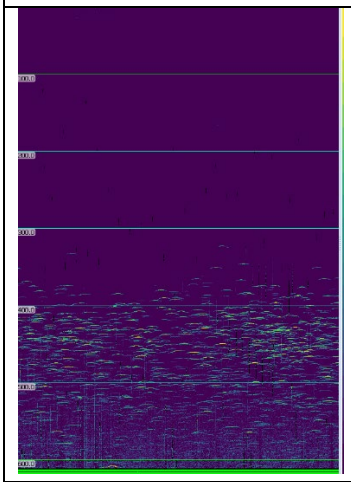

PS144_022 PSN_PS Pelagic Trawl

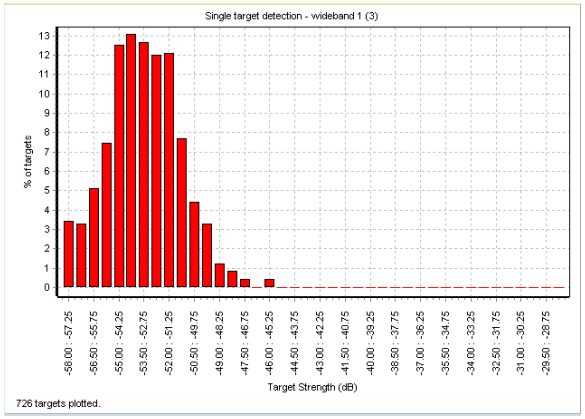

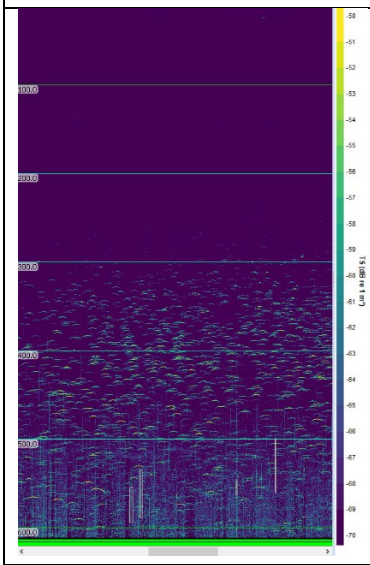

PS144_055 PSN_PS Pelagic Trawl

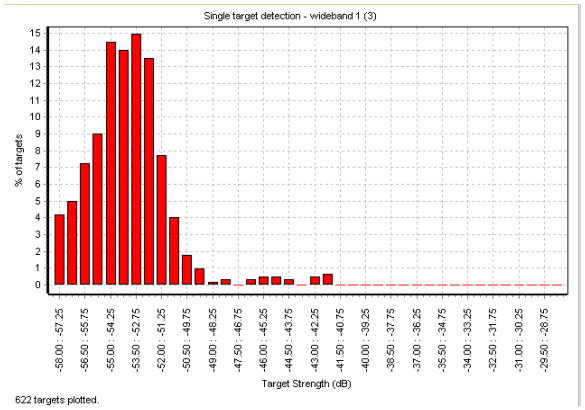

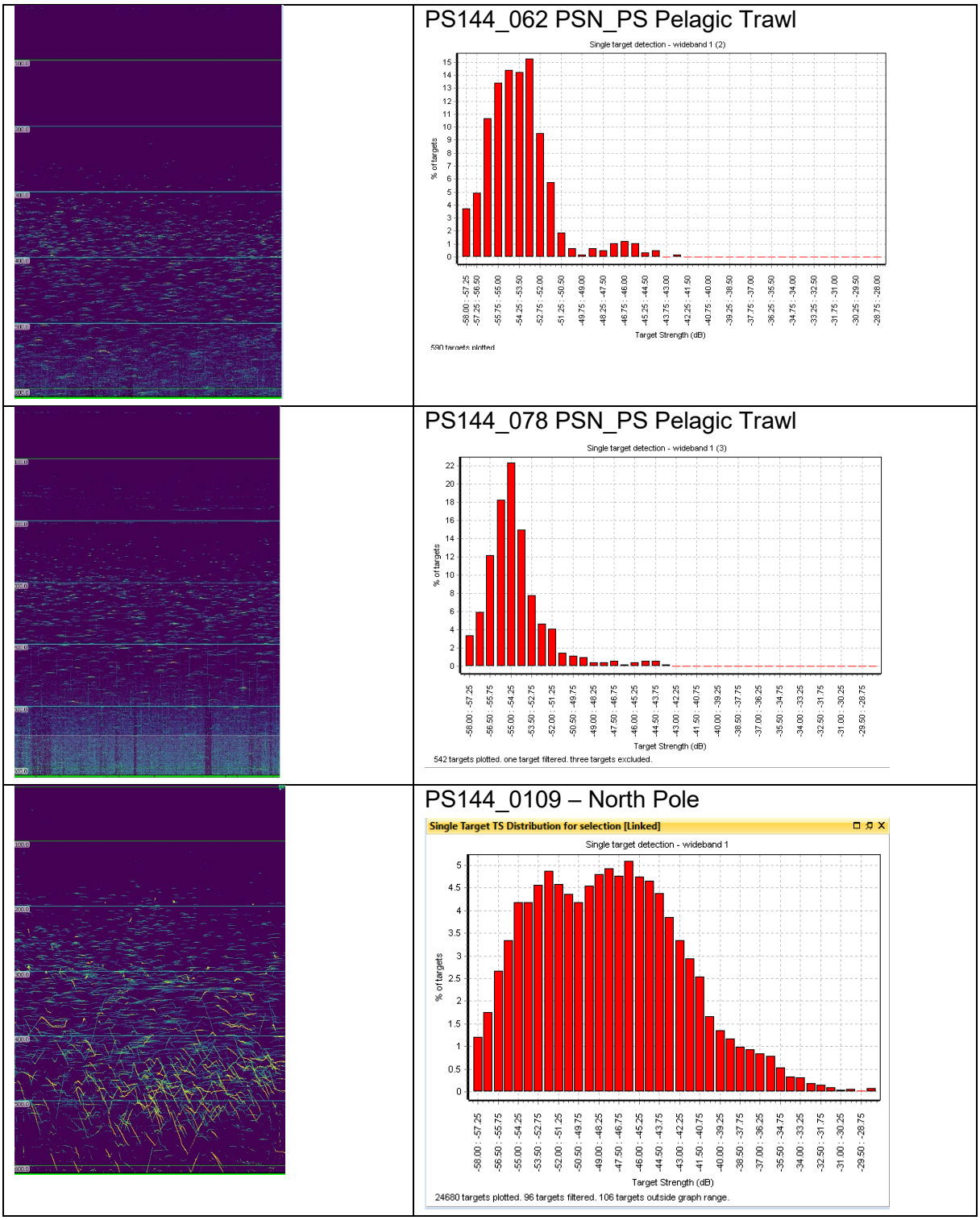

Fig. 7.13: *Examples of echograms (left) and target strength distribution (right) during deployments of the pelagic trawl, and at station 109 near the North Pole.*

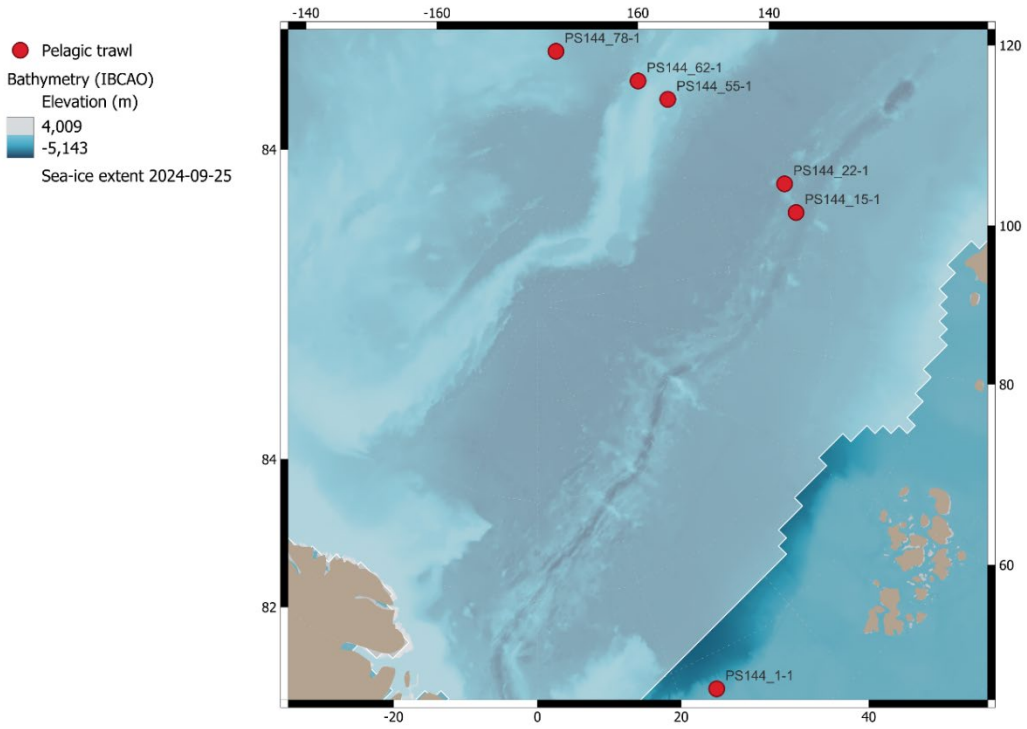

Fig. 7.14: *Distribution of pelagic trawl deployments during PS144.*

Pelagic trawl. Pelagic trawls were performed at one test station (station 1) on the Svalbard shelf break, and five stations on Transect III (Fig. 7.14). The target depth was determined based on 38 kHz backscatter profiles from the EK80. In most cases, this was the center of the DSL (300-500) m. At station 1, the DSL was absent, and we targeted a backscatter maximum at 50 m depth. At station 62, we detected several signals with target strengths indicating larger fish between 500 and 600 m (Fig. 7.13), and the fishing depth was therefore adjusted to 550 m (Table 7.8).

Altogether, the pelagic trawl caught 72 finfish, not counting larvae (Table 7.8). At station 1, the catch (19 fish) was composed of larval and juvenile fish, including horse mackerel *Trachurus trachurus*, Greenland halibut *Reinhardtius hippoglossoides*, snailfish *Liparis* sp., twohorn sculpin *Icelus bicornis*, and Gadidae (Fig. 7.15). We also caught 109 larval flatfish (Pleuronectiformes), and 16 squid larvae. On Transect III, the only fish species caught were the lanternfish *Benthosema glaciale* (44 fish) and, occasionally polar cod *Boreogadus saida* (9 fish) which was probably caught near the surface (Fig. 7.15). The invertebrate catch was dominated by the amphipod *Themisto libellula* and shrimp (mainly *Hymenodora glacialis*). At station 62 where we fished below the DSL, we caught a large number of shrimp (588) and 7 larval and 1 juvenile squid (probably *Gonatus fabricii*) over 10 cm in size (Fig. 7.16). These results suggest that the DSL in the research area was predominantly inhabited by one species *Benthosema glaciale*, at low density but with a relatively even distribution.

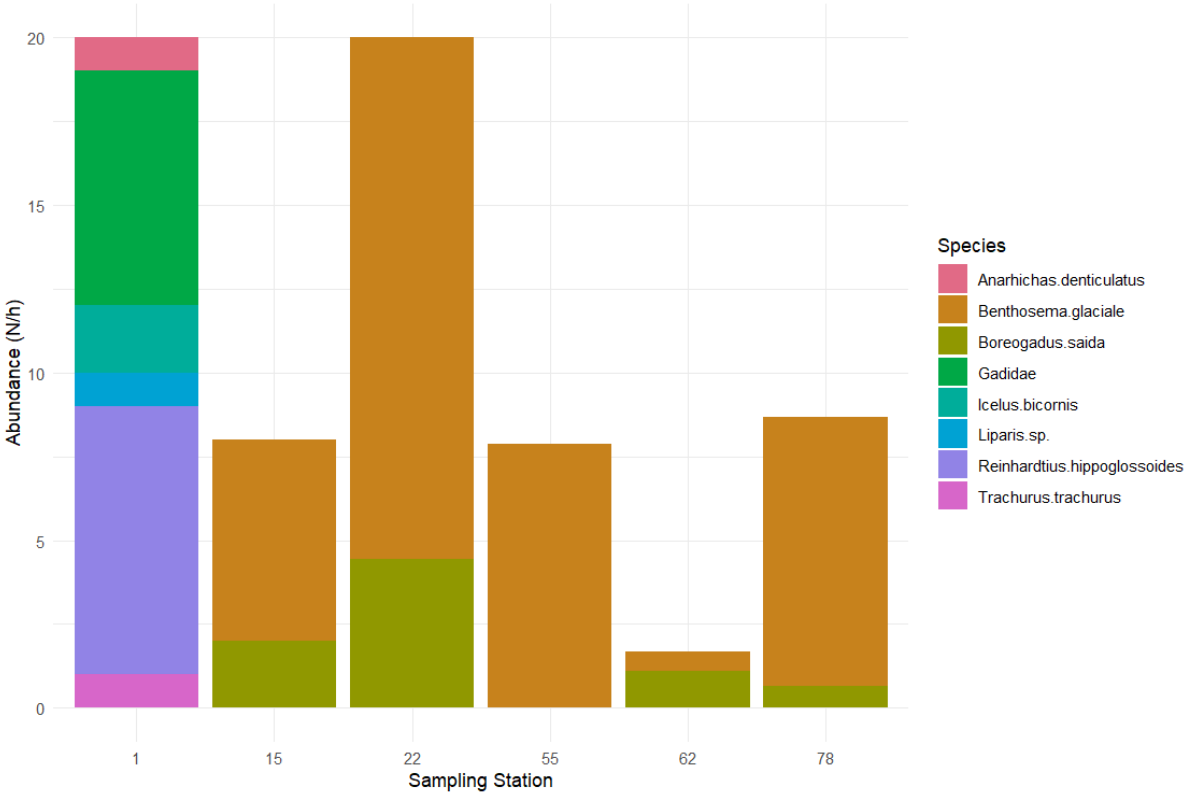

Fig. 7.15: *Taxonomic composition of finfish caught with the pelagic trawl during PS144. Abundances relative to sampling effort are expressed in numbers per hour trawled (N/h).*

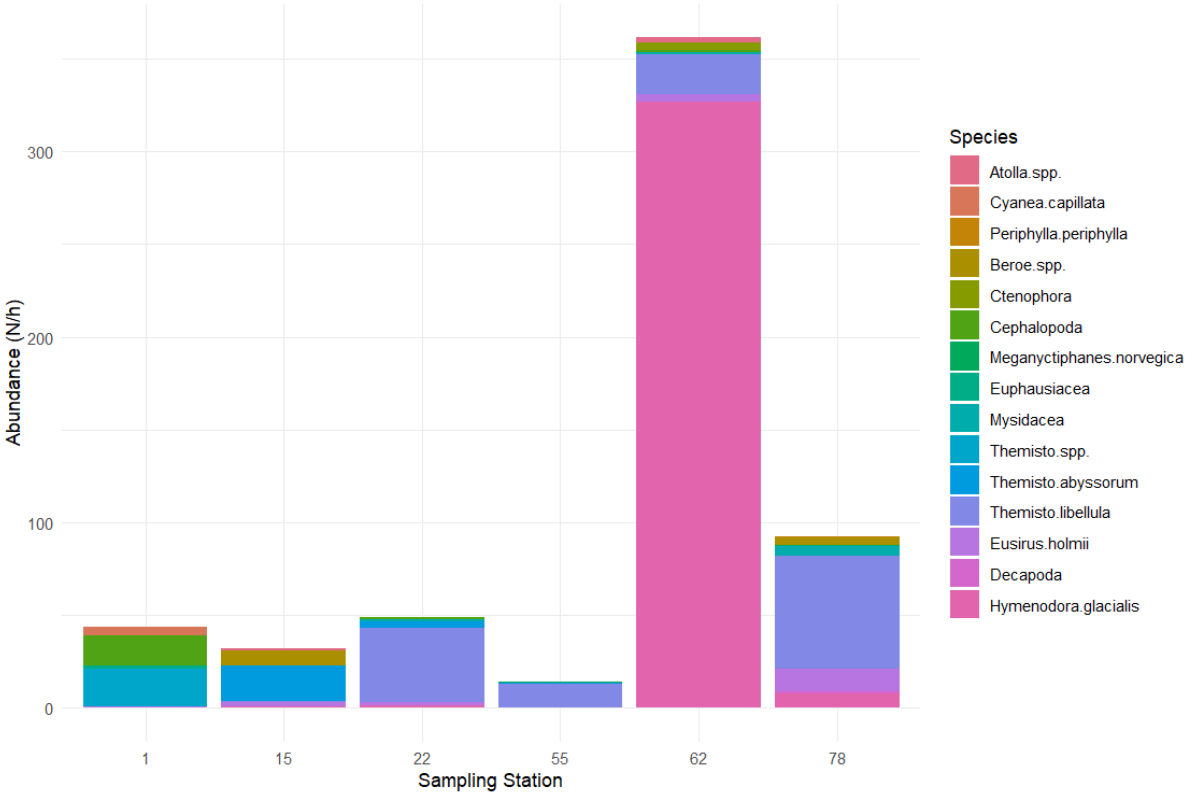

Fig. 7.16: *Taxonomic composition of invertebrates caught with the pelagic trawl during PS144. Abundances relative to sampling effort are expressed in numbers per hour trawled (N/h).*

Table 7.8: Overview of pelagic trawls conducted during PS144.

Event	Date	Latitude [°N]	Longitude [°E]	Target depth [m]	Time trawled [h]	No of fish caught
PS144_1-1	2024-08-13	81.411	25.038	50	1	19
PS144_15-1	2024-08-21	84.426	109.687	450	1	8
PS144_22-1	2024-08-29	84.414	116.132	450	0.9	18
PS144_55-1	2024-09-06	85.056	147.638	350	1.4	11
PS144_62-1	2024-09-07	85.014	155.818	550	1.8	3
PS144_78-1	2024-09-10	84.835	175.810	350	1.5	13
Total						**72**

Longlines and traps. At all “super” ice stations in transect 3 and transect 2, fishing from the ice flow were conducted. All fishing devices were deployed at the earlierst after opening the ice stations and were recovered as the latest cast on ice. Longlines were used to catch possible large predatory fish within the Atlantic water layer (Figure 7.17, 7.18). Therefore, a combination of headlines and three different longlines with 170, 130 and 230 hooks, respectively, were used to reach a maximum line length between 506 and 614 metres (Table 7.9). Due to varying and partly strong currents at depth underneath the ice the realized maximum depth of the longline could not exactly be determined. The deployment time varied between stations with a minimum of 14 and a maximum of 36.5 hours. Despite some reasonable backscatter signals in the EK80 at several stations, no fish was caught at any station. Three seperate longlines were used over time and the squid bait was frozen on the line afterwards and reused for 2 or 3 deployments. Only at ice station 4 (PS144_050_01_ICE04), severe problems occurred during recovery of the longline because of heavy load on the line or the hooks getting caught on ice ridges underneath the ice. Finally, more than 50 % of the deepest hooks were without bait, twisted or lost. Due to the long distance to the ship and other devices on the ice flow it seems unlikely that the longline got stuck by these devices and some biological activity seems likely. It remains unclear whether other large predators (e.g. seals) were responsible for this anomaly.

Fig. 7.17: *Deployment of longlines through an ice hole. The main line was coiled in a bucket and the hooks attached by a monofile line and a swivel to it were sorted in systematic order around the bucket. Pieces of squid were used as bait. Foto: Magnus Lucassen).*

Fig. 7.18: *Recovery of longlines using an electrical line hauler (Northlift LH 300). Foto: Magnus Lucassen*

To catch polar cod, a fyke net was modified to be deployed directly under the ice at three ice stations (Fig. 7.19, 7.20). Deployment times were similar to those of the longlines. Directly at the first try (ice station 4), one polar cod was caught, being in perfect condition. As we aimed to transport a number of living animals to Bremerhaven, the fish was initially kept alive in a recirculating aquarium system at 0°C. As no further intact fish were caught at a later stage of the cruise this specimen was finaly sacrified, and tissue samples were taken for ecological and transcriptomic studies.

Fig. 7.19: *Deployment of the fyke net under ice. Foto: Magnus Lucassen*

Several under-ice traps were deployed six times in conjunction with the longlines to sample ice amphipods and polar cod (Snoeijs-Leijonmalm et al. 2022). Despite adequate deployment times, no fish could be caught by this device. Even no ice amphipod found its way into the trap. The used bait (fermented fish byproducts) was used successfully for fish and amphipods throughout several expeditions to the Southern Ocean, but even bait from the the natural habitat (smashed shrimp from the RMT) did not attract more fish. Altogether, the low success of all ice fishing devices aligns to the overall low biological acitivity as observed by EK80, PSN, SUIT, RMT and multinet.

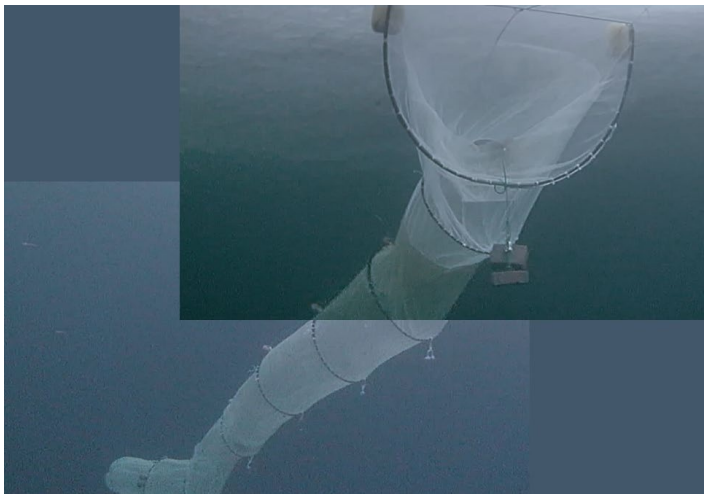

Fig. 7.20: *The fyke net under ice. Foto: Hauke Flores*

Table 7.9: Overview of fish sampling efforts at ice stations during PS144. Fk = fyke; FR = fishing rod; LL = longline

Station	Date	Lati-tude	Longi-tude	LL	No of hooks	LL length [m]	Head rope [m]	Time (h)	Fk	No of traps	FR
10	2024-08-19	85.26	83.60	-					-	-	+
23	2024-08-29	84.50	115.72	+	170	306	200	17	-	2	
50	2024-09-04 - 2024-09-05	85.03	139.94	+	170	306	290	17	+	2	
67	2024-09-08	84.95	162.09	+	130	234	330	14	-	4	
85	2024-09-12 - 2024-09-13	87.50	178.73	+	130	234	340	19	-	2	
109	2024-09-18 - 2024-09-19	89.95	-142.70	+	230	414	200	24.5	+	2	
123	2024-09-23	88.07	59.95	-				-	-		+
134	2024-09-25 - 2024-09-26	87.05	57.07	+	230	414	200	36.5	+	2	

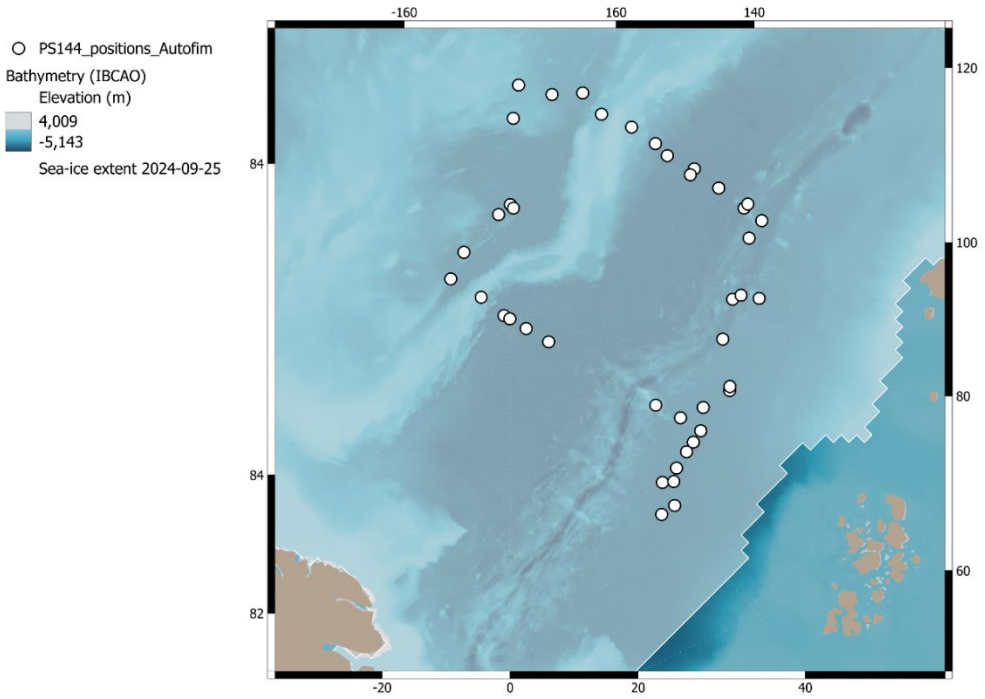

Fig. 7.21: *Distribution of AutoFim samples during PS144.*

WP3

Protist DNA. During this expedition we aimed to improve the understanding of the eukaryotic microbial community composition to address the dynamics of the cryo-pelagic coupling in biodiversity in autumn with special emphasis on the re-freezing. For this, 2000 ml of seawater for both Chlorophyl a and eukaryotic DNA analysis were taken within the upper 100 meters of the water column during 22 CTD stations (Tab. 7.1). Per CTD, samples from five water depths (100 meter, 50 meter, Surface, Chlorophyl maximum and Below chlorophyl maximum) were collected using plastic bottles. In addition, ice cores and under ice water were taken at nine ice stations using ice corers and under ice hand pumps (Tab. 7.2). Altogether, size-fractionated chlorophyll *a* and protist DNA samples were taken at 22 CTD stations and nine ice stations (Tab. 7.1, Tab. 7.2).

To create a more coherent picture, underway samples were collected using the automated and remote-controlled filtration system for marine microbes (AutoFim) (Metfies et al., 2016) (Figure 7.21, 7.22). From the 15.08.2024 until the 12.10.2024 this system took, except for some days of maintenance duration, daily water samples from ten meters depth below the ship (Table 7.10). Per run the AutoFim system collected samples at up to six filters, which were fixed with P-buffer and after being removed from the system stored at -80°C until further analysis at the AWI. Until 12 October 2024, we collected 52 AutoFim samples (Tab. 7.10).

After being collected, the 2000 ml of either seawater or under ice water were run through a size fractionated filtration using 47 mm PC membrane filter and a vacuum pump. For Chlorophyll the water was first filtered through a 3 µm filter, collected and afterwards filtered through a 0.4 µm filter. For the eukaryotic DNA the procedure was similar to the one for Chlorophyll, but at the beginning the water was filtered through a 10 µm filter, before being filtered through 3 µm and 0.4 µm filters. All filtrations were conducted under dark conditions with limited light intrusion to prevent particles from being degraded. After filtration all filters were stored at -80°C until further analysis at the AWI.

For Chlorophyll and DNA only ice from the bottom 10 cm of the ice core was used. When the core sections had melted, 1000-2000 ml of water were collected for Chlorophyll analysis and filtered as described above. The same amount of water was used for DNA analysis but filtered

on a Sterivex filter using a peristaltic pump. All samples were stored at -80°C until further analysis at the AWI.

Fig. 7.22: *The AutoFim. Foto: Jannis Hümmling*

Table 7.10: Overview of AutoFim samples taken during PS144. Transit = Transit phase, Medivac = Medivac phase, station, T I = Transect I, T II = Transect II, T III = Transect III.

Transect	**Number of samples**
Transit 1 & 2	9
Medivac	6
Transect III	15
Transect II	13
Transect I	3
Home Transit	6
Total	52

Phytoplankton diversity. To investigate phytoplankton diversity, water samples for microscopy, Imaging Flow Cytobot (IFCB), and flow cytometric analysis were collected from 2 to 5 depths (surface, chlorophyll a maximum, subsurface backscattering maximum depth, 50 m, 100 m) in the upper 100 m at 22 stations, using a 12-L PVC Niskin water sampler attached to a CTD rosette system (Table 7.11). Subsamples for ice algae were taken from the ice cores and seawater samples from under-ice water and subsurface backscattering maximum depth at 9 ice stations. To fill gaps in the geographic distribution of phytoplankton between stations, discrete water samples were also collected while underway, using the ship's seawater supply at a nominal depth of 7 m along the cruise track.

Seawater samples for IFCB analysis were collected in polypropylene bottles, fixed with glutaraldehyde (final concentration: 0.5%) for 1 hour, and stored at -20 ºC until analysis. Phytoplankton species abundance will be determined using the IFCB, which collects images of particles containing chlorophyll fluorescence in the laboratory at KOPRI (Olson and Sosik, 2007). All digital micrographs will be automatically classified using a supervised machine learning strategy (Laney and Sosik, 2014). For microscopic analysis, seawater samples from Niskin bottles were collected in polypropylene bottles, preserved with glutaraldehyde (final concentration 0.5%), and stored at -20 ºC until analysis. Sample volumes of 20 - 100 mL will be filtered through Gelman GN-6 Metricel filters (0.45 µm pore size, 25 mm diameter) to prepare microscopic slides in a water-soluble embedding medium (HPMA, 2-hydroxypropyl methacrylate) at KOPRI. The HPMA slides will be used for identification and estimation of cell

concentration and biovolume. Seawater samples for picophytoplankton were fixed for 15 min with glutaraldehyde (final concentration: 0.1%) and stored at -80 ºC until analysis. Samples will be analyzed on a Accuri C6 flow cytometer (Becton Dickinson) equipped with an air-cooled argon laser (488 nm, 15 mW) to enumerate picophytoplankton abundance at KOPRI. Picophytoplankton groups will be identified and enumerated using the characteristics of 90°-angle light scatter, orange fluorescence from phycoerythrin, and red fluorescence from chlorophyll (Marie et al., 1997). Raw data from the flow cytometer will be processed using the FlowJo program (Tree Star, www.flowjo.com).

Table 7.11: Numbers of stations sampled for phytoplankton and picophytoplankton abundance in the transect II (T II), transect III (T III), and transit section during the PS144 expedition.

		CTD	FSW	ICE	Total
Transit 1	IFCB	3	16	1	20
Transit 1	Microscope	1	7	1	9
Transit 1	FCM		13		13
Transect III	IFCB	11		5	16
Transect III	Microscope	11		5	16
Transect III	FCM	11			11
Transit 2	IFCB	1		1	2
Transit 2	Microscope	1		1	2
Transit 2	FCM	1			1
Transect II	IFCB	7		2	9
Transect II	Microscope	7		2	9
Transect II	FCM	7			7
Total IFCB		22	16	9	47
Total Microscope		20	7	9	36
Total FCM		19	13		32

Foraminifera. Fossil foraminiferal assemblages are widely used for palaeoenvironmental reconstructions. However, for the correct interpretation of fossil data, it is crucial to improve our understanding of the correlation between environmental variability in the ocean and the distribution of living planktonic foraminifera. The objective of this expedition is to sample different depth intervals within the water column to examine the abundance and distribution of planktonic foraminifera at the various water masses. Eight multinet casts with a mesh size of 55 µm were conducted to collect planktonic foraminifera (Tab. 7.4). J. Wollenburg will analyse the net samples. Expected results will provide an insight into regional understanding and calibration of climate proxy indicators used in marine geology.

Data management

Environmental data will be archived, published and disseminated according to international standards by the World Data Center PANGAEA Data Publisher for Earth & Environmental Science (https://www.pangaea.de) within two years after the end of the expedition at the latest. By default, the CC-BY license will be applied.

Molecular data (DNA and RNA data) will be archived, published and disseminated within one of the repositories of the International Nucleotide Sequence Data Collaboration (INSDC, www.insdc.org) comprising of EMBL-EBI/ENA, GenBank and DDBJ).

Any other data will be submitted to an appropriate long-term archive that provides unique and stable identifiers for the datasets and allows open online access to the data.

This expedition was supported by the Helmholtz Research Programme “Changing Earth – Sustaining our Future” Topic X, Subtopic Y.

In all publications based on this expedition, the **Grant No. AWI_PS144_06** will be quoted and the following publication will be cited:

Alfred-Wegener-Institut Helmholtz-Zentrum für Polar- und Meeresforschung (2017) Polar Research and Supply Vessel POLARSTERN Operated by the Alfred-Wegener-Institute. Journal of large-scale research facilities, 3, A119. http://dx.doi.org/10.17815/jlsrf-3-163.

References

Castellani G, Schaafsma FL, Arndt S, Lange BA, Peeken I, Ehrlich J, David C, Ricker R, Krumpen T, Hendricks S, Schwegmann S, Massicotte P, Flores H (2020) Large-Scale Variability of Physical and Biological Sea-Ice Properties in Polar Oceans. Frontiers in Marine Science 7: ARTN 536 https://doi.org/10.3389/fmars.2020.00536

Kawakami T, Yamazaki A, Jiang H-C, Ueno H, Kasai A (2023) Frontiers in Marine Science: https://doi.org/10.3389/fmars.2023.1193083

Kohlbach D, Graeve M, Lange BA, David C, Peeken I, Flores H (2016) The importance of ice algae-produced carbon in the central Arctic Ocean ecosystem: Food web relationships revealed by lipid and stable isotope analyses. Limnol Oceanogr 61: 2027-2044 https://doi.org/10.1002/lno.10351

Laney S R, Sosik H M, 2014. Phytoplankton assemblage structure in and around a massive under-ice bloom in the Chukchi Sea. *Deep-Sea Res. II*, 105**:** 30–41

Marie D, Partensky F. Jacquet S, Vaulot D, 1997. Enumeration and cell-cycle analysis of natural populations of marine picoplankton by flow cytometry using the nucleic-acid stain SYBR Green I. *Appl Environ Microb*, 14: 113-118

Metfies, K., Schroeder, F., Hessel, J., Wollschläger, J., Micheller, S., Wolf, C., Kilias, E., Sprong, P., Neuhaus, S., Frickenhaus, S., & Petersen, W. (2016). High-resolution monitoring of marine protists based on an observation strategy integrating automated on-board filtration and molecular analyses. *Ocean Science*, *12*(6), 1237–1247. https://doi.org/10.5194/os-12-1237-2016

Olson R J, Sosik H M, 2007. A submersible imaging-in-flow instrument to analyze nano- and microplankton: Imaging FlowCytobot. *Limnol. Oceanogr. Methods*, 5: 195–203

Snoeijs-Leijonmalm P, Flores H, Niehoff B, Sakinan S, Svenson A, Castellani G, Hildebrandt N (2021) Ecosystem mapping in the Central Arctic Ocean (CAO) during the MOSAiC Expedition. Final Report. European Commission. 90 pp.

Snoeijs-Leijonmalm P and the SAS-Oden 2021 Scientific Party (2022a) Expedition Report SWEDARCTIC Synoptic Arctic Survey 2021 with icebreaker Oden. Swedish Polar Research Secretariat. 300 pp.

Snoeijs-Leijonmalm P, Flores H, Sakinan S, Hildebrandt N, Svenson A, Castellani G, Vane K, Mark FC, Heuzé C, Tippenhauer S, Niehoff B, Hjelm J, Sundberg JH, Schaafsma FL, Engelmann R (2022b) Unexpected fish and squid in the central Arctic deep scattering layer. Sci Adv 8: eabj7536 https://doi.org/10.1126/sciadv.abj7536

Trueman CN, Artetxe-Arrate I, Kerr LA, Meijers AJS, Rooker JR, Sivankutty R, Arrizabalaga H, Belmonte A, Deguara S, Goñi N, Rodriguez-Marin E, Dettman DL, Santos MN, Karakulak FS, Tinti F, Tsukahara Y, Fraile I (2023) Thermal sensitivity of field metabolic rate predicts differential futures for bluefin tuna juveniles across the Atlantic Ocean. Nat Commun 14: 7379 https://doi.org/10.1038/s41467-023-41930-2

Vane K, Cobain MRD, Trueman CN, Vonnahme TR, Rokitta S, Polunin NVC, Flores H (2023) Tracing basal resource use across sea-ice, pelagic, and benthic habitats in the early Arctic spring food web with essential amino acid carbon isotopes. Limnol Oceanogr n/a https://doi.org/10.1002/lno.12315